arXiv:hep-ph/0211373v1 24 Nov 2002

NLO QCD Predictions for associated $t\bar{t}h$ production in Hadronic Collisions

S. Dawson[a] *, L. H. Orr[b] †, L. Reina[c] ‡ and D. Wackeroth[d]

[a]Physics Department, Brookhaven National Laboratory, Upton, NY 11973, USA

[b]Department of Physics and Astronomy, University of Rochester, Rochester, NY 14627, USA

[c]Physics Department, Florida State University, Tallahassee, FL 32306-4350, USA

[d]Department of Physics, SUNY at Buffalo, Buffalo, NY 14260, USA

We present the next-to-leading-order (NLO) QCD corrections to the inclusive total cross section for the production of a Higgs boson in association with a top anti-top quark pair within the Standard Model at the Tevatron and the LHC.

1. Introduction

The search for the Higgs boson of the Standard Model (SM) is one of the major tasks of the next generation of high-energy collider experiments. The direct limit on the SM Higgs boson mass, M_h, from LEP2 searches and the indirect limit from electroweak precision data strongly suggest the existence of a light Higgs boson, $M_h < 193$ GeV (95 % C.L.) [1], which may be within the reach of the Fermilab Tevatron $p\bar{p}$ collider [2]. However, since the dominant SM Higgs production channels are plagued with low event rates and large backgrounds, the Higgs boson search at the Tevatron requires high luminosity, and all possible production channels should be considered. The production of a SM Higgs boson in association with a top-quark pair, $p\bar{p} \to t\bar{t}h$, can play a role for almost the entire Tevatron discovery range [2,3]. Although the $t\bar{t}h$ event rate is small, the signature of such events is quite spectacular ($W^+W^-b\bar{b}b\bar{b}$).

At the CERN LHC pp collider, the associated $t\bar{t}h$ production mode will play a crucial role in the 110 GeV$\leq M_h \leq$130 GeV mass region both for discovery and for precision measurements of the Higgs boson couplings. This process will provide a direct measurement of the top-quark Yukawa coupling and will be instrumental in determining ratios of Higgs boson couplings in a model independent way [4]. Such measurements could help to distinguish a SM Higgs boson from more complex Higgs sectors, e.g., as predicted by supersymmetry, and shed light on the details of the generation of fermion masses.

As for any other hadronic cross section, the next-to-leading-order (NLO) QCD corrections are expected to be numerically important and are crucial in reducing the (arbitrary) dependence of the cross sections on the factorization and renormalization scales. Here we summarize the calculation of the NLO QCD predictions for associated $t\bar{t}h$ production at the Tevatron and the LHC. Results for the Tevatron have been presented in Refs. [5–8] and for the LHC in Refs. [7–9]. The results of the two groups are in very good agreement within the statistical errors.

*This work is supported in part by the U.S. Department of Energy under grant DE-AC02-76CH00016.

†This work is supported in part by the U.S. Department of Energy under grant DE-FG02-91ER40685.

‡This work is supported in part by the U.S. Department of Energy under grant DE-FG02-97ER41022.

2. QCD corrections to $t\bar{t}h$ production

The inclusive total cross section for pp (or $p\bar{p}$) $\to t\bar{t}h$ at $\mathcal{O}(\alpha_s^3)$ can be written as:

$$\sigma_{NLO}(p\overset{(-)}{p} \to t\bar{t}h) = \sum_{ij} \frac{1}{1+\delta_{ij}} \int dx_1 dx_2 \qquad (1)$$

$$\cdot[\mathcal{F}_i^p(x_1,\mu)\mathcal{F}_j^{p(\bar{p})}(x_2,\mu)\hat{\sigma}_{NLO}^{ij}(\mu) + (1 \leftrightarrow 2)] \ ,$$

where $\mathcal{F}_i^{p,\overline{p}}$ are the NLO parton distribution functions for parton i in a proton/antiproton, defined at a generic factorization scale $\mu_f = \mu$, and $\hat{\sigma}_{NLO}^{ij}$ is the $\mathcal{O}(\alpha_s^3)$ parton-level total cross section for incoming partons i and j, renormalized at an arbitrary scale μ_r. We take $\mu_r = \mu_f = \mu$. The NLO parton-level total cross section $\hat{\sigma}_{NLO}^{ij}$ consists of the $\mathcal{O}(\alpha_s^2)$ Born cross section and the $\mathcal{O}(\alpha_s)$ corrections to the Born cross section, including the effects of mass factorization. It contains virtual and real corrections to the parton-level $t\bar{t}h$ production processes, $q\bar{q} \to t\bar{t}h$ and $gg \to t\bar{t}h$, and the tree-level $(q,\bar{q})g$ initiated processes, $(q,\bar{q})g \to t\bar{t}h(q,\bar{q})$, which are of the same order in α_s. The main challenges in the calculation come from the presence of pentagon diagrams in the virtual corrections with several massive external and internal particles, and from the computation of the real part in the presence of infrared singularities.

2.1. Virtual Corrections

The calculation of the virtual corrections to the $q\overline{q}$ initiated sub-process is described in detail in Ref. [6]. The calculation of the virtual corrections to $gg \to t\bar{t}h$ is technically similar. The basic method is to reduce each virtual diagram to a sum of scalar integrals, which may contain both ultraviolet (UV) and infrared (IR) divergences. The finite scalar integrals are evaluated by using the method described in Ref. [10] and cross checked with the numerical package FF [11]. The scalar integrals that exhibit UV and/or IR divergences are calculated analytically. Both the UV and IR divergences are extracted by using dimensional regularization in $d = 4-2\epsilon$ dimensions. The UV divergences are then removed by introducing a suitable set of counterterms, as described in detail in Ref. [6] The remaining IR divergences are cancelled by the analogous singularities in the soft and collinear part of the real gluon emission cross section.

The most difficult integrals arise from the IR-divergent pentagon diagrams with several massive particles. In Refs. [5,6] we calculated the pentagon scalar integrals as linear combinations of scalar box integrals using the method of Ref. [12]. For the gg initiated process we also used the method of Ref. [10] and found perfect agreement between the results of the two methods. The virtual corrections to the gg initiated process have an additional complication with respect to the $q\bar{q}$ case because of the presence of pentagon tensor integrals with rank higher than one. Pentagon tensor integrals can give rise to numerical instabilities due to the dependence on inverse powers of the Gram determinant. The Gram determinant vanishes when two momenta become degenerate, i.e. at the boundaries of phase space. These are spurious divergences, which cause serious numerical difficulties. We have used two methods to overcome this problem and found mutual agreement within the phase space integration statistical uncertainty:

- Impose kinematic cuts to avoid the phase space regions where the Gram determinant vanishes. Then apply an extrapolation procedure from the numerically safe to the numerically unsafe region.

- Eliminate all pentagon tensor integrals by cancelling terms in the numerator against the propagators wherever possible, after interfering the pentagon amplitude with the Born-matrix element. The resulting expressions are very large, but numerically stable.

2.2. Real Corrections

The real corrections are computed using the phase space slicing (PSS) method, in both the double [13] and single [14] cutoff approaches. In both approaches the IR region of the $t\bar{t}h+g$ phase space where the emitted gluon cannot be resolved is defined as the region where the gluon kinematic invariants:

$$s_{ig} = 2p_i \cdot p_g = 2E_iE_g(1-\beta_i\cos\theta_{ig}) \qquad (2)$$

become small. Here p_i is the momentum of an external quark or gluon (with energy E_i), $\beta_i = \sqrt{1-m_i^2/E_i^2}$, p_g is the final state gluon momentum with energy E_g, and θ_{ig} is the angle between $\vec{p}_i$ and $\vec{p}_g$. In the IR region the cross section is calculated analytically and the resulting IR divergences, both soft and collinear, are cancelled, after mass factorization, against the corresponding divergences from the $\mathcal{O}(\alpha_s)$ virtual corrections.

The single cutoff PSS technique defines the IR region as that where

$$s_{ig} < s_{min} \ , \tag{3}$$

for an arbitrarily small cutoff s_{min}. The two cutoff PSS method introduces two arbitrary parameters, δ_s and δ_c, to separately define the IR soft and IR collinear regions according to:

$$\begin{aligned} &E_g < \frac{\delta_s \sqrt{s}}{2} \quad \text{soft region} \ , \\ &(1-\cos\theta_{ig}) < \delta_c \quad \text{collinear region} \ . \end{aligned} \tag{4}$$

In both methods, the real contribution to the NLO cross section is computed analytically below the cutoffs and numerically above the cutoffs, and the final result is independent of these arbitrary parameters. With this respect, it is crucial to study the behavior of σ_{NLO} in a region where the cutoff(s) are small enough to justify the analytical calculations of the IR divergent contributions to the real cross section, but not so small as to cause numerical instabilities.

This is the first application of the single cutoff phase space slicing approach to a cross section involving more than one massive particle in the final state. The numerical results of both methods agree within the statistical errors. In Ref. [7], the dipole subtraction formalism has been used to extract the IR singularities of the real part. The agreement between these three very different treatments of the real IR singularities represents a powerful check of the corresponding NLO calculations.

3. $t\bar{t}h$ production at the Tevatron

For $p\bar{p}$ collisions at $\sqrt{s}=2$ TeV, more than 95% of the tree-level cross section comes from the subprocess $q\bar{q} \to t\bar{t}h$, while the gg and $(q,\bar{q})g$ initial

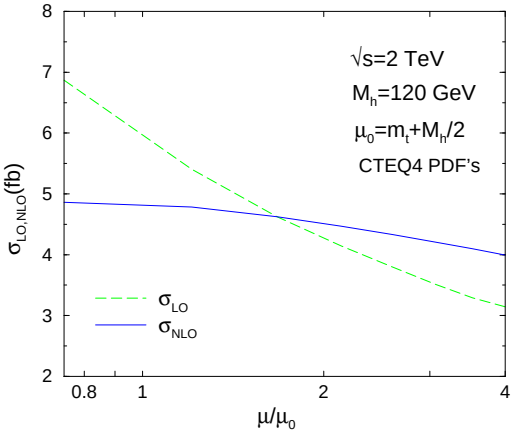

Figure 1. Dependence of $\sigma_{LO,NLO}(p\bar{p} \to t\bar{t}h)$ on the renormalization/factorization scale μ, at the Tevatron ($\sqrt{s}=2$ TeV), for $M_h=120$ GeV [5,6].

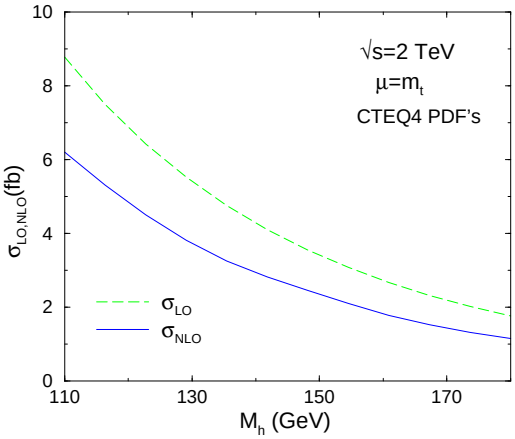

Figure 2. Dependence of $\sigma_{LO,NLO}(p\bar{p} \to t\bar{t}h)$ on M_h, at $\sqrt{s}=2$ TeV, for $\mu = m_t$ [5,6].

states are numerically irrelevant. Therefore, in [5,6], when calculating $\sigma_{NLO}(p\bar{p} \to t\bar{t}h)$ of Eq. (1), we only included the $q\bar{q} \to t\bar{t}h$ channel, summed over all light quark flavors. The NLO inclusive total cross section is shown in Figs. 1 and 2, as a function of the renormalization/factorization scale μ and as a function of the Higgs boson mass M_h, respectively. As expected, the NLO cross section at the Tevatron shows a drastic reduction in the scale dependence from the lowest order prediction. The NLO corrections reduce the total cross section by a factor of $0.7-0.95$ for $m_t < \mu < 2m_t$. Only for $\mu > 2m_t + m_h$ is the NLO cross section larger than the Born prediction.

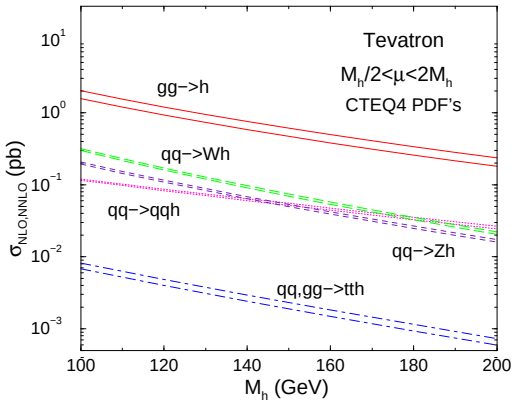

Figure 3. $\sigma_{NLO,NNLO}$ for SM Higgs production processes at the Tevatron ($\sqrt{s}$ = 2 TeV) as a function of M_h. For $p\bar{p} \to t\bar{t}h$, the renormalization/factorization scale is varied between $m_t + M_h/2 < \mu < 4(m_t + M_h/2)$.

To conclude, we want to summarize the state of the art of existing NLO and next-to-NLO (NNLO) calculations for the main SM Higgs boson production processes at the Tevatron. To this purpose, in Fig. 3 we show the renormalization/factorization scale dependence of the inclusive total cross sections at NLO (NNLO in case of $gg \to h$) for the main SM Higgs production processes. We only omit $b\bar{b}h$ associated production, since no complete NLO result is yet available. The renormalization/factorization scales are varied in the range $M_h/2 < \mu < 2M_h$ for all processes except $p\bar{p} \to t\bar{t}h$, where we varied it in the range $m_t + M_h/2 < \mu < 4(m_t + M_h/2)$. The QCD NLO calculations for the $q\bar{q} \to Wh, Zh$ [15], $qq \to qqh$ [16] and $q\bar{q} \to t\bar{t}h$ [5–7] processes provide reliable predictions for the inclusive total cross sections at the Tevatron. However, the NLO corrections to the $gg \to h$ cross section [17] are large (up to $\sim 100\%$), and the NNLO corrections, that recently became available [18,19], are crucial to obtain reliable predictions [20].

4. $t\bar{t}h$ production at the LHC

The associated production of $t\bar{t}h$ at the LHC with $\sqrt{s} = 14$ TeV is dominated at the parton level by $gg \to t\bar{t}h$, and in determining $\sigma_{NLO}(pp \to t\bar{t}h)$, the $\mathcal{O}(\alpha_s)$ corrections to the sub-process $gg \to t\bar{t}h$ provide the largest contribution. However,

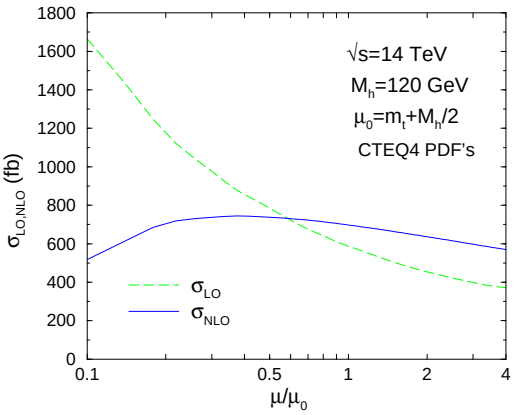

Figure 4. Dependence of $\sigma_{LO,NLO}(pp \to t\bar{t}h)$ on the renormalization/factorization scale μ, at the LHC ($\sqrt{s}$=14 TeV), for M_h=120 GeV [9].

the other partonic channels cannot be neglected, and in calculating $\sigma_{NLO}(pp \to t\bar{t}h)$ of Eq. (1), we included all sub-processes, initiated by gg, $q\bar{q}$, and $(q, \bar{q})g$ [9].

The scale dependence of $\sigma_{NLO}(pp \to t\bar{t}h)$ at $\sqrt{s} = 14$ TeV is also strongly reduced compared to the LO result, as can be seen in Fig. 4. The variation of $\sigma_{NLO}(pp \to t\bar{t}h)$ with the SM Higgs mass is shown in Fig. 5, for $\mu = 2m_t + M_h$. At the LHC, the NLO QCD corrections enhance the LO cross section by a factor of $1.2 - 1.4$ over the entire range of values of the renormalization/factorization scale shown in Fig. 4, and over the relevant Higgs boson mass interval shown in Fig. 5.

Finally, as we did for the Tevatron in Fig. 3, we summarize in Fig. 6 the state of the art of existing NLO and next-to-NLO (NNLO) calculations for the main SM Higgs boson production processes at the LHC.

5. Conclusion

The inclusive cross section for $p\bar{p}, pp \to t\bar{t}h$ has been calculated at NLO of QCD, and the theoretical uncertainty on its prediction has been drastically reduced to 10-15% for the Tevatron and to 15-20% for the LHC.

The availability of this NLO result as well as the recent calculation of the NNLO correction to inclusive Higgs production, allows us to summa-

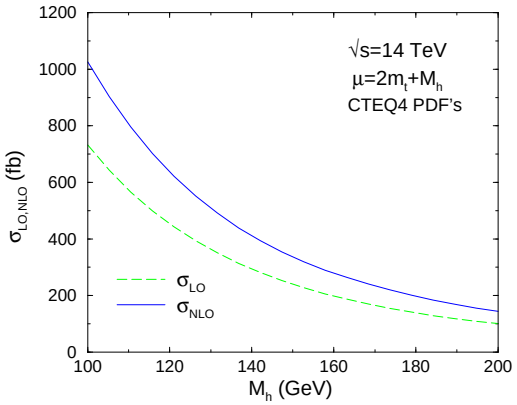

Figure 5. Dependence of $\sigma_{LO,NLO}(pp \to t\bar{t}h)$ on M_h, at $\sqrt{s}=14$ TeV, for $\mu=2m_t+M_h$ [9].

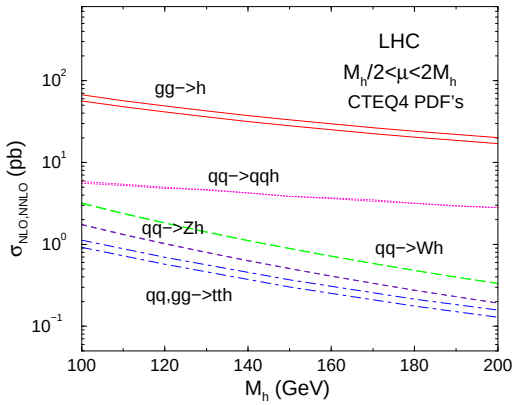

Figure 6. $\sigma_{NLO,NNLO}$ for SM Higgs production processes at the LHC ($\sqrt{s}=14$ TeV) as a function of M_h. For $pp \to t\bar{t}h$, the renormalization/factorization scale is varied between $m_t+M_h/2<\mu<4(m_t+M_h/2)$.

rize the state of the art of higher order calculation for Higgs boson production cross sections at both the Tevatron and the LHC. The theoretical predictions for Higgs boson production at the Tevatron and the LHC are well understood at NLO, and except for the $gg \to h$ process, for which the NNLO corrections are mandatory, the arbitrary scale dependence at NLO is small.

Acknowledgments

We thanks the Authors of Ref. [7] for a detailed comparison of the results.

REFERENCES

1. D. Abbaneo *et al.* [LEPEWWG], hep-ex/0112021; M. W. Grunewald, arXiv:hep-ex/0210003.
2. M. Carena and H. E. Haber, hep-ph/0208209.
3. J. Goldstein *et al.*, Int. J. Mod. Phys. A **16S1A**, 308 (2001); Phys. Rev. Lett. **86**, 1694 (2001).
4. A. Belyaev and L. Reina, JHEP **0208**, 041 (2002); D. Zeppenfeld, hep-ph/0203123.
5. L. Reina and S. Dawson, Phys. Rev. Lett. **87**, 201804 (2001).
6. L. Reina, S. Dawson, and D. Wackeroth, Phys. Rev. D **65**, 053017 (2002).
7. W. Beenakker, S. Dittmaier, M. Krämer, B. Plümper, M. Spira, and P. M. Zerwas, Phys. Rev. Lett. **87**, 201805 (2001).
8. S. Dittmaier, these proceedings, hep-ph/0210380.
9. S. Dawson, L. H. Orr, L. Reina, and D. Wackeroth, BNL-HET-02/27, FSU-HEP-2002-1115, UB-HET-02-09.
10. A. Denner, Fortsch. Phys. **41**, 307 (1993).
11. G. J. van Oldenborgh and J.A. Vermaseren, *Z. Phys.* **C46**, 425 (1990).
12. Z. Bern, L. Dixon, and D. A. Kosower, Phys. Lett. B **302**, 299 (1993) [Erratum-ibid. B **318**, 649 (1993)]; Nucl. Phys. B **412**, 751 (1994).
13. For a review see, e.g., B. W. Harris and J. F. Owens, Phys. Rev. D **65**, 094032 (2002).
14. W. T. Giele, E. W. Glover and D. A. Kosower, Nucl. Phys. B **403**, 633 (1993), S. Keller and E. Laenen, Phys. Rev. D **59**, 114004 (1999).
15. T. Han and S. Willenbrock, Phys. Lett. B **273**, 167 (1991).
16. T. Han, G. Valencia, and S. Willenbrock, Phys. Rev. Lett. **69**, 3274 (1992).
17. S. Dawson, Nucl. Phys. B **359**, 283 (1991); A. Djouadi, M. Spira, and P. M. Zerwas, Phys. Lett. B **264**, 440 (1991).
18. R. V. Harlander and W. B. Kilgore, Phys. Rev. Lett. **88**, 201801 (2002);
19. C. Anastasiou and K. Melnikov, hep-ph/0207004.
20. We thank the authors of [18] for providing the NNLO results.